

Research Article

Research and Deduction of Car-to-TW Vehicle AEB Test Scenarios Based on Improved Clustering Methods

Xinchi Dong ¹, **Qiaoyu Zhang**,² **Daowen Zhang** ^{1,3,4}, **Chaojian Wang**,¹
and **Tianshu Zhang**⁵

¹*School of Automobile and Transportation, Xihua University, Chengdu 610039, China*

²*Department of Transportation, Southwest Jiaotong University Hope College, Chengdu 610400, China*

³*Vehicle Measurement Control and Safety Key Laboratory of Sichuan Province, Xihua University, Chengdu 610039, China*

⁴*Provincial Engineering Research Center for New Energy Vehicle Intelligent Control and Simulation Test Technology of Sichuan, Xihua University, Chengdu 610039, China*

⁵*Engineering, Computer and Mathematical Sciences, The University of Adelaide, North Terrace, Adelaide, SA 5005, Australia*

Correspondence should be addressed to Daowen Zhang; 0119910025@mail.xhu.edu.cn

Received 12 January 2023; Revised 3 September 2023; Accepted 3 October 2023; Published 13 October 2023

Academic Editor: Yajie Zou

Copyright © 2023 Xinchi Dong et al. This is an open access article distributed under the Creative Commons Attribution License, which permits unrestricted use, distribution, and reproduction in any medium, provided the original work is properly cited.

Two-wheeled (TW) vehicle accidents are one of the major types of urban traffic accidents. TW cyclists who lack safety protection usually suffer more serious injuries and deaths in collisions. Developments in automotive active safety technologies are expected to reduce cyclist injuries and deaths, such as automatic emergency braking (AEB). To facilitate the development and testing of AEB technology, typical TW vehicle scenarios need to be constructed. Based on 400 cases of car-to-TW vehicle accident data from the National Automobile Accident In-Depth Investigation System (NAIS) database, we investigated the scenario elements that influence AEB robustness, such as weather, accident time, and road wetness. We obtained seven static scenarios using an improved clustering method, and we obtained specific speed and distance combinations in each scenario using a deduction method. Further, we compared the present findings to those of other scholars and the China New Car Assessment Program (C-NCAP). The kinematic states of the two were similar to that of C-NCAP, but the speed distribution was significantly different. The TW vehicle speed in the C-NCAP is set to 15 km/h or 20 km/h concerning the European test scenarios, but the TW vehicle speed in the present study was 10–60 km/h. Thus, the present findings recommended that subsequent C-NCAP test scenarios increase the category of motorcycles and the speed range of cars covering 20–70 km/h and consider the test conditions of bad weather and wet roads, to test the robustness of AEB.

1. Introduction

Two-wheeled (TW) vehicles, such as bicycles, electric two-wheelers, and TW motorcycles, have become a common means of transportation for Chinese individuals due to their advantages of low cost, lightness, flexibility, and ease of operation. As of 2017, there were 370 million TW vehicles in China [1]. TW vehicles provide convenience but also have some safety problems. According to the statistics of the last five years, there are approximately 200,000 traffic accidents in China every year, among which the number of traffic accidents related to TW vehicles is more than 50,000 [1].

Moreover, car-to-TW vehicle accidents have become the most common type of traffic accidents in China [2]. Compared to drivers of cars, drivers of TW vehicles, as vulnerable users of road traffic, often suffer more serious injuries in collisions [3], indicating the continual need to pay attention to traffic problems associated with TW vehicles.

With the development and application of automatic emergency braking (AEB) technology, hazardous traffic scenarios involving TW vehicles have become one of the important directions of research on the safety of self-driving vehicles [4–6]. AEB uses radar to measure the distance to the vehicle in front of an obstacle, and when the detected

distance is less than the safe distance, it will reduce the collision speed by automatically braking to avoid a collision or reduce the severity of a collision. Studies have shown that AEB significantly reduces the severity of pedestrian and TW vehicle accidents [7, 8]. The AEB technologies developed by each vehicle manufacturer have different performance standards, indicating the need for a standard assessment method to test the safety of AEB. The Euro New Car Assessment Program (Euro NCAP) first introduced an AEB test scenario for pedestrians in 2016, followed by an AEB test scenario for TW vehicles in 2018 (Euro NCAP, 2019) [9]. Considering the traffic differences in China, the China New Car Assessment Program (C-NCAP) introduced the AEB test scenarios for pedestrians and TW vehicles in 2018 and 2021, respectively (C-NCAP, 2021) [10].

However, the test scenarios of these standards and regulations involve relatively single elements and working conditions, making it difficult to cover complex road traffic conditions. Before introducing an evaluation scheme for AEB, test scenarios need to correspond to actual traffic scenarios [11]. Moreover, not all scenarios are equally important. More typical scenarios have higher safety benefits for testing AEB technology [12]. Using descriptive statistics based on accident data is one of the common methods to obtain typical scenarios. For example, Camp et al. [13] used descriptive statistics to construct the most common car-to-TW vehicle AEB test scenarios based on the Community Database on Accidents on the Roads in Europe and formulated a test protocol. Sui et al. [14] used a similar approach to discover the most common accident scenarios in China based on accident data from the China in-depth accident study (CDAS), providing a reference for the construction of car-to-TW vehicle AEB test scenarios in China.

In addition, there is heterogeneity in traffic data, and the homogeneity of the same group of data cannot be guaranteed by descriptive statistics, suggesting that some wrong conclusions may be obtained [15]. Clustering is an unsupervised classification method that alleviates the problem of heterogeneity among data groups by dividing data objects into homogeneous multiple groups through the inherent similarity of the dataset [15]. Currently, clustering analysis has been applied to build the car-to-TW vehicle AEB test scenario. For example, Cao et al. [16] constructed four car-to-TW vehicle AEB test scenarios using cluster analysis based on 216 accidents in the National Automobile Accident In-Depth Investigation System (NAIS) database considering seven scenario elements, such as roadway, passenger vehicle speed, and the TW vehicle form of motion. However, these scenarios did not consider scenario elements, such as weather and blind spots in the field of view, resulting in the constructed scenarios not being effective in testing the robustness of the AEB. Sui et al. [17] obtained six categories of typical TW vehicle AEB test scenarios using cluster analysis based on 672 accident data from the CDAS, with full consideration of scenario elements, such as weather and blind areas of vision. However, Sui et al. treated all two-wheelers as one category, resulting in a lack of significant differences in the characteristics of these scenarios.

In most previous studies that constructed car-to-TW vehicle AEB test scenarios based on cluster analysis, the importance of the variable categories was the same. However, the degree of influence of each type of variable should be different for the perception, decision, and execution layers of the AEB technology. The static and dynamic variables of scene descriptions were mostly centralized in previous studies, thus affecting the sample similarity within the cluster. In addition, the obtained typical scenarios generally only described the static parameters of the scene, such as the traffic environment situation and the form of conflict between traffic participants, without meticulously involving the perception-related parameters, such as the type of TW vehicle, the state of cyclists, and the danger boundary between speed and distance. At the same time, domestic and foreign scholars use natural driving data to mine typical hazard scenarios, requiring tens of thousands of kilometers of collection miles to obtain a small number of hazardous conditions, and problems, such as insufficient hazard data samples and high costs, exist when mining typical scenarios. In contrast, the use of traffic accident typical feature parameters to build hazard scenarios has relatively better coverage and low-cost features. Thus, the present study aimed to obtain static scenarios based on accident data with video records in the NAIS database, using an improved clustering method that considers the importance of variables, and to derive the hazard thresholds of the main kinematic parameters of both parties involved by constructing dynamic parameter models, effectively covering the discrete hazard data extracted directly from traffic accidents, and realizing the extended exploration of unknown hazard scenarios to obtain typical AEB test scenarios.

2. Methods

2.1. Data. Compared to natural driving data, traffic accident data have good feasibility and coverage. In addition, the use of the typical feature parameters of traffic accidents to construct hazard scenarios has relatively better coverage and low cost. The data in the present study were obtained from the NAIS database, which was established by the Defective Products Management Center of Administration of Quality Supervision, Inspection, and Quarantine in addition to several university vehicle accident research institutes and traffic forensic centers in China. The NAIS database is one of the most abundant databases available in China, and it combines the characteristics of traffic accidents and is representative of traffic accident scenario research in China. The accident areas include plain areas, mountainous areas, plateau areas, and coastal areas. The collected accidents have the characteristics of traffic accidents in different geographical environments in China, and the accident data include the basic variables of traffic accidents, such as time, location, age, gender, and degree of injury [4].

To obtain representative data on major traffic accidents in China and better reflect the significance of improving vehicle safety, NAIS has developed strict data collection requirements, which include three parts, namely, data collection, analysis data, and relevant analysis reports, as well as

detailed descriptions of each road traffic accident collected. As of 2021, the NAIS database has collected data on 6,000 traffic accidents. Only passenger car-to-TW vehicle accidents were considered in the present study, using the following selection criteria: (1) the accident was caused by a collision between a passenger car and a TW vehicle only; (2) the passenger car types included sedan, sport utility vehicles (SUVs), and multipurpose vehicles (MPVs); (3) the two-wheeler types included TW motorcycles, TW electric vehicles, and bicycles; (4) the case information had to have computer-aided design (CAD) process diagrams drawn or video information providing the motion process of the two participants before the collision; and (5) the information on the variables involved in the cases was complete or could be determined by converting the information collected from other cases. Based on these requirements, 400 cases of compliant passenger car-to-TW vehicle accidents were selected from the database.

2.2. Selection of Clustering Variables. The original data in NAIS comprehensively describe the basic information of the whole accident process, but they also include some duplicate description data, incomplete description data, and missing data. Therefore, the selection work for the scene fields and the organization of the data of the selected fields are important before the clustering analysis. In the present study, the selection of scenario variables was mainly based on the importance of perception, decision-making, and execution of AEB as the starting point, and the fields were considered around the road environment conditions, vehicle conditions of both participants, and personnel factors of the vulnerable participants. The categories, descriptions, and reasons for the selected variables are shown in Table 1. Instead of using the velocity variable as a clustering variable, the present study utilized the quartile method to count the velocities of various static scenarios, and it combined the extrapolation method to obtain the specific distances of various scenarios.

2.3. Improved Clustering. Clustering is the process of dividing data objects into groups or clusters based on the inherent similarity of the dataset. The hierarchical clustering algorithm is one of the most widely used clustering methods [18], which refers to the creation of a hierarchical decomposition of a given set of data objects into trees with a hierarchical structure or clusters. The algorithm is simple and easy to understand, and the distance and similarity rules are easy to define. Moreover, there are few constraints, and the tree diagram contains information regarding the entire algorithm process. In addition, the algorithm allows hierarchical relationships of the classes to be identified. However, the computational time complexity of this method is high, and the singular values may have a large impact on the results. Therefore, the aim of the present study was to improve on the basis of hierarchical clustering.

In clustering, distance is generally used to evaluate the similarity between samples or classes. In previous studies, the effect of all types of variables on AEB was the same. However, in real traffic environments, the four components

of road, environment, car, and TW vehicle have different levels of influence on the perception, decision, and execution levels of AEB. Therefore, in the present study, we selected the absolute value distance to improve the distance calculation of the sample by adding the weight of the variables to allow the weighted absolute distance to solve the problem of the different importance of the variables [19]. The present study used the validated weighted absolute distance method to calculate the distance between samples as described below.

Let the 400 samples be x_1, x_2, \dots, x_{400} , and then, the distance between the i th sample x_i and the j th sample x_j is defined as the sum of the distances between all fields of the two samples. A weighting factor α_k is introduced to apply the weights of each of the variables obtained from the fuzzy comprehensive evaluation to the traditional absolute value distance. The calculation formula for weighted absolute distance is as follows:

$$d_{ij} = \sum_{k=1}^n \alpha_k |x_{ik} - x_{jk}|, \quad (1)$$

where d_{ij} is the distance between sample x_i and sample x_j ; x_{ik} is the k th variable of the sample x_i ; x_{jk} is the k th variable of the sample x_j ; n is the total number of variables selected; and α_k is the weighting coefficient.

The methods used for calculating between-class distance include the minimum distance method, maximum distance method, middle distance method, and average linkage method. The average linkage method utilizes the information between all samples [20, 21]. The calculation formula for between-class distance is as follows:

$$D_{KL}^2 = \frac{1}{m_L m_K} \sum_{x_i \in G_K, x_j \in G_L} d_{ij}, \quad (2)$$

where D_{KL}^2 represents the squared distance between class G_K and class G_L ; m_K represents the number of samples in class G_K ; and m_L represents the number of samples in class G_L .

To maintain a small number of representative clustering results, the number of clusters was first determined using an inconsistency coefficient. As the number of clusters increases, if the inconsistency coefficient shows a substantial increase in the latter clusters compared to the former clusters, the former clusters are more effective [22].

2.4. Clustering Variable Weights. Because it is difficult to determine the weights of the four parts in the car-to-TW vehicle scenarios with traditional methods, fuzzy synthetic evaluation was used [23], which involved four steps that are described as follows.

For Step 1, the set of evaluation elements was established according to the main influences of each part on AEB [24, 25] using the following formula:

$$\begin{aligned} U &= \{u_1, u_2, u_3\} \\ &= \{\text{Perception layer, decision - making layer, execution layer}\}. \end{aligned} \quad (3)$$

TABLE 1: Variable specification.

| Category | Variable | Description | Reason for clustering |
|-------------|--------------|--|---|
| Road | Dry/wet | Wet and dry conditions of the road surface, including dry and wet | Different road types have an impact on the implementation of different collision avoidance strategies, while the dry and wet conditions of the road surface have an impact on the ground adhesion coefficient |
| | TYPE_R | Types of road, including crossroads, T-intersection, and ordinary roads | |
| Environment | Obstruct | Whether the TW has a blind spot to car | Environmental factors can have an impact on the radar and cameras of autonomous vehicles |
| | Weather | Weather conditions, including sunny, cloudy, and severe weather | |
| | Time | The time of the accident, including daytime, nighttime, and morning-evening | |
| Car | TYPE_Car | Types of cars, including sedan and nonsean (SUV, MPV) | Different types of cars affect where sensors are installed, and the car's precrash driving behavior affects the active safety system's decision-making |
| | BEHAVIOR_Car | The driving behavior of car, including straight, left, and right | |
| TW | TYPE_TW | Types of TW, including traditional bicycles, electric TWs, and motorcycles | As an identification target, the type and physical appearance of the TW have an impact on the identification and tracking of the active safety system |
| | BEHAVIOR_TW | The driving behavior of TW, including straight, left, and right | |
| | Relative | The direction of motion of TWs relative to cars, including incoming traffic from the left (Left), incoming traffic from the right (Right), traveling in the same direction (Same), and traveling in opposite directions (Opposite) | |
| | Helmet | Whether the driver of a TW wears a helmet | |

For Step 2, the single-level sequencing method was used. According to the importance of the above evaluation elements [26, 27], the weight coefficients of each evaluation element were established using the following formula:

$$\begin{aligned} A &= \{a_1, a_2, a_3\} \\ &= \{0.5, 0.3, 0.2\}. \end{aligned} \quad (4)$$

For Step 3, the benchmarks and corresponding value quantities were evaluated using the following formula:

$$\begin{aligned} V &= \{v_1, v_2, v_3, v_4\} \\ &= \{\text{Very important, important, fairly important, least important}\} \\ &= \{0.4, 0.3, 0.2, 0.1\}. \end{aligned} \quad (5)$$

For Step 4, fuzzy synthetic evaluation is conducted. The relationship between the four main parts of the scenario variables, the car safety system, and the opinions of experts in the field of scenario research were comprehensively considered.

By summarizing the opinions of experts, a summary table of the investigation of the important factors of the variables in the two-wheel collision scene is obtained. Then, according to the proportion of the number of options to the total number of experts, the single-factor fuzzy evaluation table for the importance of variables is obtained, as shown in Table A1 (Supplemental File, Appendix). Finally, the weights of each part were calculated based on the affiliation matrix of each part, and the weights were normalized.

3. Results

3.1. Weighted Result. Based on the scoring results, the affiliation matrix R of each part was obtained using the following formulas (equations (6)–(9)):

$$R_{TW} = \begin{bmatrix} 0.86 & 0.14 & 0 & 0 \\ 0.29 & 0.71 & 0 & 0 \\ 0.29 & 0.29 & 0.14 & 0.29 \end{bmatrix}, \quad (6)$$

$$R_{Car} = \begin{bmatrix} 0.43 & 0.14 & 0.14 & 0.29 \\ 0.57 & 0.29 & 0 & 0.14 \\ 0.43 & 0.43 & 0.14 & 0 \end{bmatrix}, \quad (7)$$

$$R_{Road} = \begin{bmatrix} 0.29 & 0.43 & 0.29 & 0 \\ 0.14 & 0.57 & 0.29 & 0 \\ 0.29 & 0.29 & 0.43 & 0 \end{bmatrix}, \quad (8)$$

$$R_{Environment} = \begin{bmatrix} 0.71 & 0.29 & 0 & 0 \\ 0.29 & 0.57 & 0 & 0.14 \\ 0.29 & 0.29 & 0.14 & 0.29 \end{bmatrix}. \quad (9)$$

Considering the weight coefficients of the above evaluation elements, FSE was performed for each part. The comprehensive affiliation vector B is shown in the following equations (equations (10)–(13)):

$$\begin{aligned} B_{TW} &= A \times R_{TW} \\ &= \{0.5, 0.3, 0.2\} \times \begin{bmatrix} 0.86 & 0.14 & 0 & 0 \\ 0.29 & 0.71 & 0 & 0 \\ 0.29 & 0.29 & 0.14 & 0.29 \end{bmatrix} \\ &= \{0.575, 0.341, 0.028, 0.058\}. \end{aligned} \quad (10)$$

In the same way,

$$\begin{aligned} B_{Car} &= A \times R_{Car} \\ &= \{0.472, 0.243, 0.098, 0.187\}, \end{aligned} \quad (11)$$

$$\begin{aligned} B_{Road} &= A \times R_{Road} \\ &= \{0.245, 0.444, 0.318, 0\}, \end{aligned} \quad (12)$$

$$\begin{aligned} B_{Environment} &= A \times R_{Environment} \\ &= \{0.5, 0.374, 0.028, 0.1\}. \end{aligned} \quad (13)$$

The combined evaluation value N of each part was calculated using the following equation:

$$\begin{aligned} N_{TW} &= B_{TW} \times V^T \\ &= (0.575, 0.341, 0.028, 0.058) \times \begin{pmatrix} 0.4 \\ 0.3 \\ 0.2 \\ 0.1 \end{pmatrix} \\ &= 0.3437. \end{aligned} \quad (14)$$

In the same way, $N_{Car} = 0.3$, $N_{Road} = 0.2948$, and $N_{Environment} = 0.3278$.

After normalization, the weights of each part were as follows: $W_{TW} = 0.27$, $W_{Car} = 0.24$, $W_{Road} = 0.23$, and $W_{Environment} = 0.26$.

3.2. Number of Categories. Figure 1 shows the inconsistency coefficient diagram. In the last few clusterings, the inconsistency coefficient of the 394th clustering was greatly improved compared to the 393rd clustering, which indicated that the 393rd clustering (the penultimate 7th clustering) was better. Thus, the final clustering was determined as seven scenarios.

3.3. Clustering Results. Table 2 shows the values and diagrams of the static parameters for each static scenario (the percentages in parentheses are the percentages of the values taken by the variables). In Scenario No. 2, the static parameters were as follows: the TW vehicle was going straight; the TW vehicle and car were traveling in the same direction; the type of TW vehicle was electric two-wheeler; the driver of the TW vehicle was not wearing a helmet; car was going straight, the type of car was a sedan; the type of road was ordinary; the road surface was dry; there was no blind spot in the field of view outside the car; the weather was sunny; and the accident occurred during daytime.

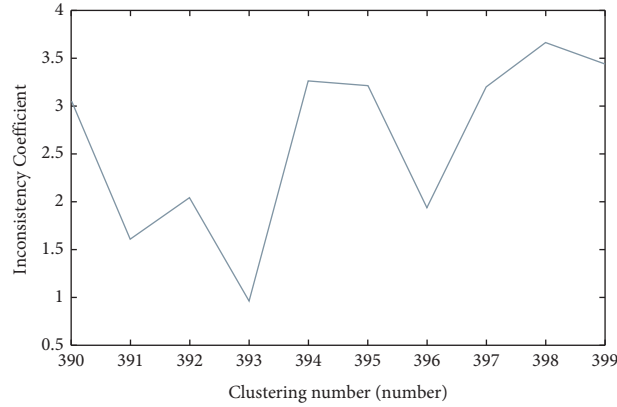


FIGURE 1: Inconsistency coefficient.

Scenarios Nos. 3, 4, 6, and 7 were all scenarios in which a car collided with a TW vehicle driving in the opposite direction. In Scenario No. 3, the frequency of clustering at crossroads and the ordinary road was the same. In Scenario No. 6, the frequency of clustering in daytime and nighttime was the same. Thus, two subscenarios were obtained for Scenario Nos. 3 and 6.

Of all the scenarios, only Scenario No. 5 involved a perpendicular collision between a car and a TW vehicle, most of which occurred at a wet intersection during the daytime.

3.4. Deduction of Dynamic Parameters. Table 3 shows the reference to the dimensions of cars and TW vehicles. To deduce the dynamic parameter combinations for seven scenarios, kinematic modeling assumptions were made. Considering the detection range of common car sensors, it was assumed that the velocities of the car (V_1) and TW vehicle (V_2) were constant before the collision, and the distance from the front end of the car to the center of the estimated collision area in each scenario was 30 m. This moment was used as the initial motion time of the scenario. The shapes of the car and TW vehicle were not particles. When studying the collision parameters, the width of the TW vehicle (a), the length of the TW vehicle (b), the width of the car (A), and the length of the car (B) were considered simultaneously.

Figure 2 shows the motion states of the two parties involved in Scenario No. 1. In this scenario, the car and the TW vehicle were driving in the same direction. The car turned right, and the TW vehicle was going straight.

When the velocity of the TW was slightly higher but not enough to avoid the car, the front end of the car collided with the rear end of the TW vehicle. The kinematic formula of the car and the TW vehicle concerning time was established as follows:

$$\frac{X_1 + S - (a/2)}{V_1} = \frac{X_{2\min} + (A/2) + b}{V_2}. \quad (15)$$

When the velocity of the car was slightly higher but not enough to avoid the TW vehicle, the front end of the TW vehicle collided with the rear end of the car. The kinematic formula of the car and the TW vehicle concerning time was established as follows:

$$\frac{X_1 + S + (a/2) + B}{V_1} = \frac{X_{2\max} - (A/2)}{V_2}, \quad (16)$$

where the distance between the front end of the car and the center of the estimated collision area is $X_1 + S = 30$ (m), and the values of a , b , A , and B are set according to the values in the table.

Because the distance X_2 from the TW vehicle to the center of the estimated collision area is an important parameter in AEB, the range of X_2 was discussed in Scenario No. 1. Combining equations (15) and (16), the relationship among V_1 , V_2 , and X_2 was obtained, in which the dangerous range of X_2 and X_{2d} was calculated using the following equation:

$$0 \leq X_{2\min} \leq X_{2d} \leq X_{2\max}. \quad (17)$$

The interquartile ranges were referenced to exclude outliers and maintain maximum coverage. The lower quartile of the car speed corresponding to each scenario was taken as the lower limit of V_1 , and the upper quartile of the car speed corresponding to each scenario was taken as the upper limit of V_1 . The lower quartile of the speed of the TW vehicle corresponding to each scenario was taken as the lower limit of V_2 , and the upper quartile of the speed of the TW vehicle corresponding to each scenario was taken as the upper limit of V_2 (Figures A1–A6 for box plots of each scenario, Supplemental File, Appendix).

Figure 3 shows the dangerous area in Scenario No. 1, in which the lower surface is the function image of $X_{2\min}$ and the upper surface is the function image of $X_{2\max}$. These two surfaces represent the boundaries of the dangerous area in Scenario No. 1, and the different degrees of danger were not considered. All combinations of velocity and distance between the two curved surfaces were considered dangerous. If emergency measures are not taken within the dangerous area of these combinations, collisions will inevitably occur.

TABLE 2: Car-to-TW vehicle static scenarios.

| Scenario | | No. 1 | No. 2 | No. 3 | No. 4 |
|-------------|--------------|------------------------------|------------------------------|-----------------------------------|-----------------------------|
| Category | Variable | | | | |
| Road | DRY/WET | Dry (94.4%) | Dry (97.6%) | Dry (100%) | Wet (93.8%) |
| Environment | TYPE_R | Crossroads (41.7%) | Ordinary roads (39.5%) | Crossroads/ordinary roads (33.3%) | Ordinary roads (37.5%) |
| | OBSTRUCT | No (97.2%) | No (85%) | Yes (100%) | No (93.8%) |
| Car | WEATHER | Sunny (83.3%) | Sunny (73.8%) | Sunny (93.3%) | Severe weather (87.5%) |
| | TIME | Daytime (69.4%) | Daytime (60.5%) | Daytime (53.3%) | Daytime (37.5%) |
| TW | TYPE_Car | Nonsedan (80.6%) | Sedan (74.1%) | Sedan (60%) | Sedan (75%) |
| | BEHAVIOR_Car | Right (77.8%) | Straight (94.8%) | Straight (93.3%) | Straight (100%) |
| RELATIVE | TYPE_TW | Electric TW vehicles (77.8%) | Electric TW vehicles (44.8%) | Motorcycles (73.3%) | Motorcycles (56.3%) |
| | BEHAVIOR_TW | Straight (91.7%) | Straight (69.6%) | Left (66.7%) | Left (68.8%) |
| HELMET | Same (75%) | Same (31.5%) | Opposite (60%) | Opposite (81.3%) | |
| Diagram | | | | | |
| Category | Variable | | | | |
| Road | DRY/WET | Wet (100%) | Dry (92.3%) | Dry (75%) | Dry (75%) |
| Environment | TYPE_R | Crossroads (52.9%) | Crossroads (38.5%) | Ordinary roads (75%) | Ordinary roads (75%) |
| | OBSTRUCT | No (88.2%) | No (100%) | Yes (100%) | Yes (100%) |
| Car | WEATHER | Severe weather (82.4%) | Sunny (84.6%) | Sunny (50%) | Sunny (50%) |
| | TIME | Daytime (70.6%) | Daytime/nighttime (42.3%) | Nighttime (100%) | Nighttime (100%) |
| TW | TYPE_Car | Nonsedan (70.6%) | Sedan (73.1%) | Sedan (100%) | Sedan (100%) |
| | BEHAVIOR_Car | Straight (70.6%) | Left (88.5%) | Straight (75%) | Straight (75%) |
| RELATIVE | TYPE_TW | Electric TW vehicles (70.6%) | Motorcycles (88.5%) | Electric TW vehicles (100%) | Electric TW vehicles (100%) |
| | BEHAVIOR_TW | Straight (82.4%) | Straight (96.2%) | Straight (75%) | Straight (75%) |
| HELMET | Left (70.6%) | Opposite (69.2%) | Opposite (50%) | Opposite (50%) | |
| Diagram | | | | | |

TABLE 3: Reference to the dimensions of cars and TW vehicles.

| | TYPE_Car | Length (unit: m) | Width (unit: m) |
|-----|---|------------------|-----------------|
| Car | Sedan (refer to SAIC Volkswagen 2019 three-model Santana) | 4.48 | 1.71 |
| | Nonsedan (reference Changan Auchan Keshan 2019 MPV) | 4.84 | 1.86 |
| TW | Traditional bicycle (reference permanent brand 24-inch leisure model bicycle) | 1.67 | 0.56 |
| | Electric TW (reference Alma electric two-wheelers, model TDR302Z) | 1.57 | 0.65 |
| | Motorbike (reference Wuyang-Honda Motorcycle (Guangzhou) Co., Ltd., model WH100T-M) | 1.9 | 0.64 |

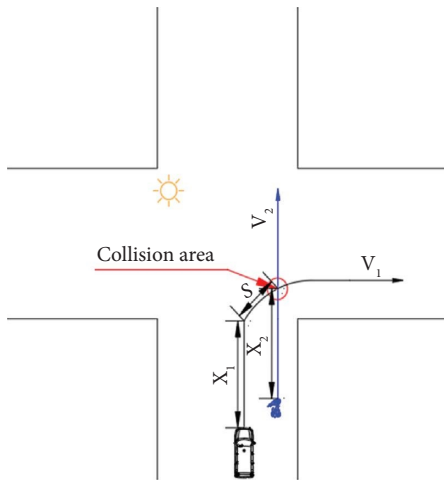


FIGURE 2: Scenario no. 1.

Figure 4 shows the dangerous area in Scenario No. 2, in which the surface (X_{2min}) is the boundary of the dangerous area in Scenario No. 2. The different degrees of danger were not considered, and the case of a TW vehicle rear-ending a car was also not considered. This surface and all combinations of velocity and distance upward along the Z-axis were considered dangerous. If emergency measures are not taken within these dangerous combinations, collisions are bound to occur.

Figures 5–8 illustrate the dangerous areas for Scenario Nos. 3, 4, 5, and 6, respectively. Figure 9 shows the motion states of the two participants in Scenario No. 7. If two participants collided in this scenario, it must have been caused by one of the participants going against traffic. Through the verification of the relevant cases, it is known that the TW vehicle traveling against traffic at nighttime is the cause of the accident, and in this case, if both participants do not slow down or both do not turn, an accident is bound to happen.

Table 4 provides the dangerous ranges of speed and distance for both parties involved in each scenario. For example, in Scenario No. 1, the dangerous range for the speed of the car was 21–40 km/h, while the dangerous range for the speed of the TW vehicle was 10–20 km/h. Moreover, the dangerous distance from the TW vehicle to the center of the collision was 5–34 m.

4. Discussions

In previous studies, scenarios were obtained using cluster analysis [17, 28]. Most scholars have treated the static and dynamic variables of the scenarios in a unified manner or treated the variable weights in the same manner in cluster analysis, thus affecting the differentiation between scenarios

and the similarity of elements within scenarios, leading to the absence of some key scenarios [4]. In addition, most scholars have not sufficiently considered the scenario variables and/or meticulously involved the type of TW vehicle, the state of the rider, and the perception-related parameters, such as speed and distance. In the present study, the scenario variables were divided into static and dynamic variables before clustering analysis, and weighted absolute distance was introduced to assign weights to each part of the static variables, which solved the problem of the unified processing of variables and the same weight of variables. Based on static scenarios, the dangerous thresholds of speed and distance for both participating parties were obtained by deduction, thereby providing specific parameter combinations of speed and distance for AEB test scenarios.

Development of the typical AEB system test scenarios seems extremely important, especially due to the huge number of TW vehicles in the road traffic in China. However, due to the road environment, traffic characteristics, and driver behaviors being different, applying the results to the different countries may not be obvious, as succinctly mentioned by other scholars [17, 28]. In the closed field test, it is equally important to select representative test scenarios. Appropriate test scenarios can produce reliable test results and reduce testing costs. Based on the accident database of the representative NAIS, this paper discovers the most common accident scenarios in China and enriches the library of car-to-TW vehicle AEB test scenarios. Uittenbogaard et al. [13] conducted descriptive statistics based on road traffic accident data in Europe and designed five car-to-TW vehicle AEB test scenarios. The source data for these scenarios related only to serious injuries and fatal accidents, and they did not consider general accidents. However, for test scenarios, both serious and fatal accidents, as well as minor injuries and accidents, should be referenced in general. In the present study, all accident scenarios were fully considered when using cluster analysis. The present study used 13 variables for description, fully considering the scenario construction elements, including important parameters, such as road type, dry road conditions, wet road conditions, and speed values characterizing the motion state of the TW vehicle, in addition to most of the study variables [17]. The two most common scenarios studied by Sui et al. were as follows: (1) two participants on a road with no blind spots in their daytime field of view in a perpendicular collision; and (2) a daytime collision between a car turning right and a TW vehicle traveling straight ahead on a road with no blind spot in the field of

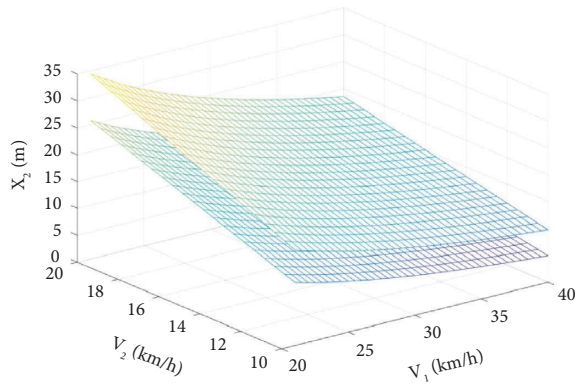


FIGURE 3: Dangerous area in Scenario No. 1.

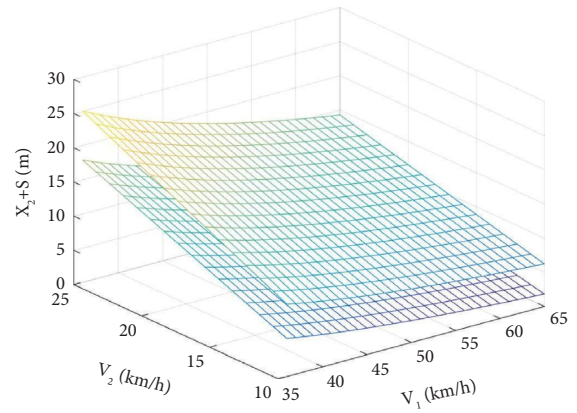


FIGURE 6: Dangerous area in Scenario No. 4.

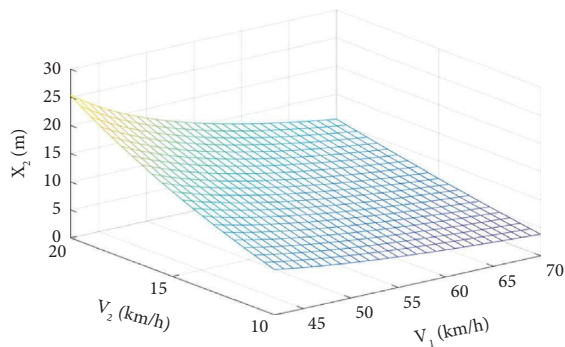


FIGURE 4: Dangerous area in Scenario No. 2.

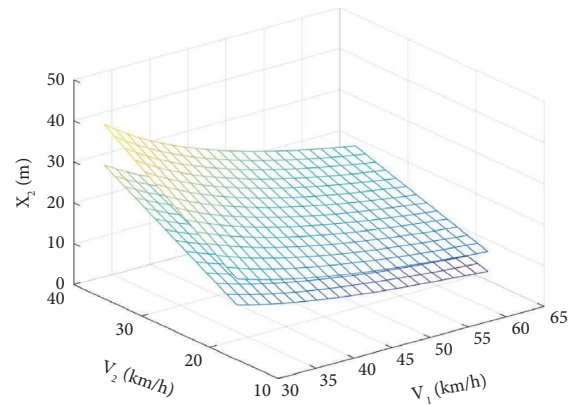


FIGURE 7: Dangerous area in Scenario No. 5.

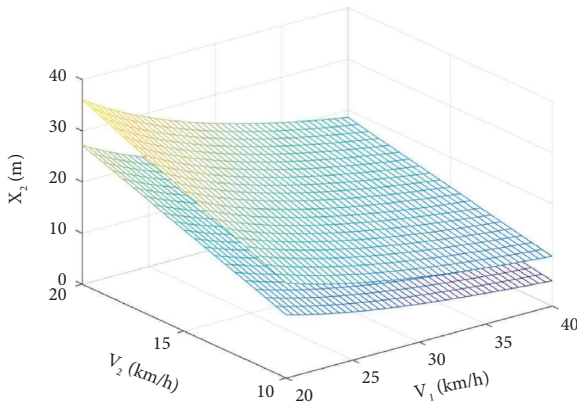


FIGURE 5: Dangerous area in Scenario No. 3.

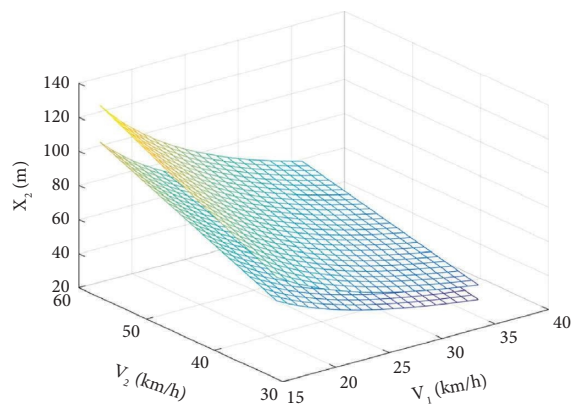


FIGURE 8: Dangerous area in Scenario No. 6.

view, with the point of collision on the right side of the car [17]. In the present study, all of these scenarios were included in the set of scenarios, and the differences in some scenarios may be due to different data or different choices of variables.

In the present study, seven car-to-TW vehicle AEB test scenarios were finally obtained using NAIS data. Among the scenarios, Scenario No. 2 had the same kinematic state as the CBLA-50 test scenario in the C-NCAP, and Scenario No. 5 had the same kinematic state as the CSFA-50 test scenario in C-NCAP (C-NCAP, 2021) [10]. In terms of static parameters, differences in weather, the wet/dry state of the road

surface, and light conditions affect the perceptual layer of AEB. However, the car-to-TW vehicle AEB test scenarios in the C-NCAP only consider daytime and dry road surfaces, and they do not consider testing under unfavorable conditions, such as nighttime or rain, preventing complete robustness testing of AEB. In the present study, two of the seven scenarios occurred on wet pavement, and two scenarios occurred at night. Therefore, different lighting and weather conditions should be considered when developing

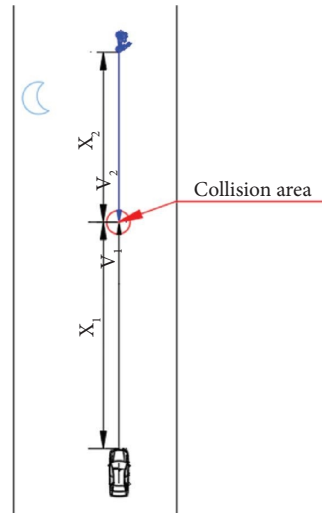


FIGURE 9: Scenario No. 7.

TABLE 4: Dangerous range of each scenario.

| Category | Scenario | | | | | | |
|-----------------|--|---|--|--|--|--|---|
| | No. 1 | No. 2 | No. 3 | No. 4 | No. 5 | No. 6 | No. 7 |
| Dangerous range | V_1 : 21–40 km/h V_2 : 10–20 km/h X_2 : 5–34 m | V_1 : 44–70 km/h V_2 : 10–20 km/h — | V_1 : 40–65 km/h V_2 : 10–26 km/h $X_2 + S$: 2–23 m | V_1 : 37–64 km/h V_2 : 10–15 km/h $X_2 + S$: 2–15 m | V_1 : 30–64 km/h V_2 : 18–36 km/h X_2 : 6–43 m | V_1 : 18–35 km/h V_2 : 34–60 km/h X_2 : 26–117 m | V_1 : 50–72 km/h V_2 : 16–50 km/h — |

test scenarios. Regarding the dynamic parameters, all four types of test scenarios in the C-NCAP for car-to-TW vehicles set the speed of the TW vehicle at 15 km/h or 20 km/h (15 km/h for bicycles and 20 km/h for electric two-wheelers), but in the Chinese traffic environment, mopeds (speeds greater than 20 km/h and less than 50 km/h) account for most TW accidents. The speed of TW vehicles in China's traffic environment easily exceeds 20 km/h or even 50 km/h when the target vehicle is a motorcycle. Therefore, in the subsequent TW vehicle AEB test scenarios in the C-NCAP, it is recommended that the speed range for electric TW vehicles be adjusted to 20–50 km/h and that the test scenarios for motorcycles be added. The suggested speed range of TW vehicles covers the 10–60 km/h range. Comparing the results of the study with those of other research scholars can verify the accuracy and reference value of the results to a certain extent from the same results and better results to make up for the shortcomings of insufficient validation in this paper. The results can be further validated in subsequent studies by drawing on advanced evaluation criteria [29].

Validation of dangerous scenarios was difficult in the present scenario evaluation because most of the previous studies on dangerous scenarios have not been fully and effectively validated. At present, two methods are used to test AEB systems: virtual and closed field tests [30]. Among them, the reliability of virtual test results depends on the selection of test scenarios as well as the accuracy of simulated vehicles and environments; while the closed field test has higher costs, it is difficult to determine the typical scenarios

and other issues are the important development direction of hazardous scenario validation and the focus of subsequent research. The weights of variables in the improved clustering method used in the present study were highly influenced by the subjective factors of experts, which is a limitation. In addition, the accident data collected by NAIS were not yet sufficient and complete. Thus, additional research on these typical cases can be conducted as the size of the database increases.

5. Conclusions

The present study was based on 400 cases of car-to-TW vehicle accident data in the NAIS database. Using the proposed hazard scenario acquisition method, seven types of typical car-to-TW vehicle hazard scenarios suitable for China's road traffic conditions were obtained, and the hazard scenario set was deduced to provide a reference for AEB test scenarios. The main conclusions were as follows:

- (1) By expert scoring and the fuzzy synthetic evaluation method, fuzzy weighting was assigned to the scene parameter categories, and the weight values of the two-wheeler situation, car situation, road situation, and environment situation were obtained as 0.27, 0.24, 0.23, and 0.26, respectively.
- (2) Improved hierarchical clustering was proposed, and the concept of weighted absolute distance was introduced. The weighted clustering was combined with the fuzzy comprehensive evaluation results to

obtain seven types of typical car-to-TW vehicle hazard scenarios that meet the road traffic conditions in China, including two TW vehicles traveling in the same direction as cars, four TW vehicles traveling in opposite directions, and one TW vehicle traveling in perpendicular direction. The static characteristics of the corresponding hazard scenarios were summarized.

- (3) Based on the seven types of hazard scenarios obtained by clustering, the kinematic model and dynamic parameter boundaries of each type of scenario were discussed. Moreover, the danger areas of each hazardous scenario were obtained.

As the speed characteristics of electric two-wheelers and motorcycles were fully considered, the kinematic states of these test scenarios were similar to those of the C-NCAP, but the speed distribution of car-to-TW vehicles was different. The speed of the TW vehicle in the C-NCAP is set to 15 km/h or 20 km/h with reference to the European test scenarios. However, the speed of the TW vehicle in the present study was 10–60 km/h. Thus, it is recommended that subsequent C-NCAP test scenarios increase the category of motorcycles and the speed range of cars covering 20–70 km/h and consider the test conditions of bad weather and wet roads, to test the robustness of AEB.

Data Availability

The article includes some data to support the results of this research. In order to protect the privacy and security of the Chinese NAIS database, NAIS restricted other information. This information can be obtained from NAIS for researchers who meet the criteria for accessing confidential data.

Conflicts of Interest

The authors declare that there are no conflicts of interest regarding the publication of this paper.

Acknowledgments

Thanks for the data support provided by the NAIS database and the China-PCS, as well as the project funding of Vehicle Measurement Control and Safety Key Laboratory of Sichuan Province (QCCK2021-011) and the State Administration of Market Administration Project (202248).

Supplementary Materials

Table A1: Single-factor fuzzy evaluation table for the importance of variables. Figure A1: Scenario No. 1. Figure A2: Scenario No. 2. Figure A3: Scenario No. 3. Figure A4:

Scenario No. 4. Figure A5: Scenario No. 5. Figure A6: Scenario No. 6. (*Supplementary Materials*)

References

- [1] A. H. Liu and Z. C. Ye, *China Statistical Yearbook—2020*, China Statistics Press, Beijing, China, 2020.
- [2] L. C. Zhang, Q. Miao, and D. D. Geng, “Research on car and two-wheeler accident characteristic analysis and object detection factor,” *Automobile Technology*, vol. 3, pp. 41–44, 2020.
- [3] H. Zhou, F. Liu, P. Li, Z. Aihong, T. Zhengping, and H. Wenhao, “Impact of electric bicycles’ roll angle on cyclist’s head injury,” *China Safety Science Journal*, vol. 29, no. 5, pp. 79–84, 2019.
- [4] Z. Tan, Y. Che, L. Xiao, W. Hu, P. Li, and J. Xu, “Research of fatal car-to-pedestrian precrash scenarios for the testing of the active safety system in China,” *Accident Analysis & Prevention*, vol. 150, Article ID 105857, 2021.
- [5] X. Yang, Y. Zou, and L. Chen, “Operation analysis of freeway mixed traffic flow based on catch-up coordination platoon,” *Accident Analysis & Prevention*, vol. 175, Article ID 106780, 2022.
- [6] Y. Jiang, F. Zhu, Z. Yao, Q. Gu, and B. Ran, “Platoon intensity of connected automated vehicles: definition, formulas, examples, and applications,” *Journal of Advanced Transportation*, vol. 2023, Article ID 3325530, 17 pages, 2023.
- [7] L. Hou, J. Duan, W. Wang, R. Li, G. Li, and B. Cheng, “Drivers’ braking behaviors in different motion patterns of vehicle-bicycle conflicts,” *Journal of Advanced Transportation*, vol. 2019, Article ID 4023970, 17 pages, 2019.
- [8] E. M. Rosen, “Autonomous emergency braking for vulnerable road users,” in *Proceedings of the 2013 International IRCOBI Conference on the Biomechanics of Injury*, Gothenburg, Sweden, September 2013.
- [9] EuroNCAP, *European New Car Assessment Programme—Test Protocol AEB VRU Systems*, Euro NCAP, Leuven, Belgium, 2019.
- [10] C-NCAP, *C-NCAP Management Regulation*, C-NCAP, Berlin, Germany, 2021 edition, 2021.
- [11] L. Li, X. C. Zhu, Y. Liu, and Z. X. Ma, “Typical traffic risk scenarios related to pedal cyclists,” *Journal of Tongji University*, vol. 42, no. 7, pp. 1082–1087, 2014.
- [12] U. Sander and N. Lubbe, “The potential of clustering methods to define intersection test scenarios: assessing real-life performance of AEB,” *Accident Analysis & Prevention*, vol. 113, pp. 1–11, 2018.
- [13] O. Opden Camp, S. van Montfort, J. Uittenbogaard, and J. Welten, “Cyclist target and test setup for evaluation of cyclist-autonomous emergency braking,” *International Journal of Automotive Technology*, vol. 18, no. 6, pp. 1085–1097, 2017.
- [14] B. Sui, S. Zhou, X. Zhao, and N. Lubbe, “An overview of car-to-two-wheeler accidents in China: guidance for AEB assessment,” in *Proceedings of 25th International Technical Conference on the Enhanced Safety of Vehicles (ESV)*, Detroit, MI, USA, June, 2017.
- [15] D. Nilsson, M. Lindman, T. Victor, and M. Dozza, “Definition of run-off-road crash clusters—for safety benefit estimation

- and driver assistance development,” *Accident Analysis & Prevention*, vol. 113, pp. 97–105, 2018.
- [16] Y. Cao, L. Xiao, H. Dong et al., “Typical pre-crash scenarios reconstruction for two-wheelers and passenger vehicles and its application in parameter optimization of AEB system based on NAIS database,” in *Proceedings of 26th International Technical Conference on the Enhanced Safety of Vehicles (ESV)*, Eindhoven, Netherlands, June 2019.
- [17] B. Sui, N. Lubbe, and J. Bärghman, “A clustering approach to developing car-to-two-wheeler test scenarios for the assessment of Automated Emergency Braking in China using in-depth Chinese crash data,” *Accident Analysis & Prevention*, vol. 132, Article ID 105242, 2019.
- [18] G. X. Zuo and C. Huang, *Data Analysis Lab Tutorial*, Central China Normal University Press, Wuhan, China, 1 edition, 2015.
- [19] M. L. Wei and R. Y. Liu, “Distance of absolute value with weight and its applications,” *Journal of Baoji University of Arts and Sciences*, vol. 2, pp. 122–124, 2007.
- [20] X. Q. He, *Multivariate Statistical Analysis*, People’s University of China Press, Beijing, China, 2008.
- [21] T. Balashanmugam, K. Sengottaiyan, M. S. Kulandairaj, and H. Dang, “An effective model for the iris regional characteristics and classification using deep learning alex network,” *IET Image Processing*, vol. 17, no. 1, pp. 227–238, 2023.
- [22] Z. H. Xie, *MATLAB Statistical Analysis and Applications: 40 Case Studies*, Beihang University Press, Beijing, China, 1 edition, 2010.
- [23] X. Sun, X. Zhu, K. Zhang, L. Li, Z. Ma, and D. Wang, “Automatic detection method research of incidents in China-FOT database,” in *Proceedings of 2016 IEEE 19th International Conference on Intelligent Transportation Systems*, Rio de Janeiro, Brazil, November 2016.
- [24] S. Feng, Y. Feng, X. Yan, S. Shen, S. Xu, and H. X. Liu, “Safety assessment of highly automated driving systems in test tracks: a new framework,” *Accident Analysis & Prevention*, vol. 144, Article ID 105664, 2020.
- [25] W. Liu, L. Wei, and Y. Li, “Occluded street objects perception algorithm of intelligent vehicles based on 3D projection model,” *Journal of Advanced Transportation*, vol. 2018, Article ID 1547276, 11 pages, 2018.
- [26] Z. J. Wang, *Transportation Systems Engineering*, Southeast University Press, Jiangsu, China, 2013.
- [27] Y. Y. Cao, “Multi-object optimizing algorithm of single ordering of hierarchy base on ant algorithm,” *Bulletin of Science and Technology*, vol. 29, pp. 10–13, 2013.
- [28] D. Pan, Y. Han, Q. Jin, H. Wu, and H. Huang, “Study of typical electric two-wheelers pre-crash scenarios using K-medoids clustering methodology based on video recordings in China,” *Accident Analysis & Prevention*, vol. 160, Article ID 106320, 2021.
- [29] J. Ge, H. Xu, J. Zhang, Y. Zhang, D. Yao, and L. Li, “Heterogeneous driver modeling and corner scenarios sampling for automated vehicles testing,” *Journal of Advanced Transportation*, vol. 2022, Article ID 8655514, 14 pages, 2022.
- [30] L. Yang, Y. Yang, G. Wu et al., “A systematic review of autonomous emergency braking system: impact factor, technology, and performance evaluation,” *Journal of Advanced Transportation*, vol. 2022, Article ID 1188089, 13 pages, 2022.